Q. J. R. Meteorol. Soc. (1999), **125**, pp. 2239–2264

Equilibrium atmospheres of a two-column radiative–convective model

By J. NILSSON[1]* and K. A. EMANUEL[2]
[1]*University of Stockholm, Sweden*
[2]*Massachusetts Institute of Technology, USA*

(Received 29 January 1998; revised 2 December 1998)

SUMMARY

Interaction between steady, large-scale atmospheric circulations and a radiative–convective environment is considered. As a model tool, we use a two-column radiative–convective model with an explicit hydrological cycle that uses clear-sky conditions in the radiation calculation. A flow field is calculated by the linearized, hydrostatic equations of motion in a non-rotating frame of reference. Mechanical damping is represented by vertical diffusion of momentum and surface drag. The flow advects heat and moisture, and thereby modifies the local radiative–convective equilibrium. A dynamically passive ocean mixed layer is situated below the model atmosphere.

All externally specified parameters are identical in the two columns, implying that local radiative–convective equilibrium is a steady solution. For weak mechanical damping (or small column length), the local equilibrium is generally unstable due to a positive feedback between large-scale subsidence and infrared cooling, which operates via advective drying. A circulating equilibrium, in which the air ascends in one column and descends in the other, is attained. Due to a reduced content of clear-sky water vapour, which is the major infrared absorber in the model, the circulating equilibrium can emit the absorbed solar radiation at a significantly lower surface temperature than the corresponding local equilibrium.

In the limit of a nearly inviscid atmosphere, the intensity of the large-scale circulation is controlled chiefly by the mid-tropospheric radiative cooling in the downdraught column. In this regime, we find two distinct equilibria with circulation that are distinguished by the features of the downdraught column: one branch with deep convection but where the integrated convective heating vanishes due to evaporation of precipitation; and one branch with shallow (or no) convection where the surface boundary layer is disconnected from the free atmosphere.

KEYWORDS: Idealized model Tropical dynamics

1. INTRODUCTION

One-dimensional radiative–convective models delineate the broad structure of planetary atmospheres. Much of our present, theoretical understanding of the climate of the earth stems from such models. Here, we consider a simple extension of a one-dimensional radiative–convective model to a side-by-side two-column model. Primarily, our motivation is to understand fundamental aspects of feedbacks between large-scale circulation, clear-sky water vapour, and infrared radiation in an idealized model. At the heart of the model is a radiative–convective code with an explicit hydrological cycle that is described by Rennó *et al.* (1994a). We assume clear skies in the radiation calculation and have chosen the simplest form of linear dynamics; the circulation is governed by hydrostatic and non-rotating equations of motion. Our model represents a maritime atmosphere overlying an ocean mixed layer.

The two-column model concept provides the simplest possible tool to investigate the interaction between large-scale flows and an environment strongly controlled by radiative and convective processes. It is instructive to distinguish between transient and steady interactions. Generally, the former interaction can be understood in linear terms while the latter type of interaction is inherently nonlinear.

Propagation of waves through an environment close to radiative–convective equilibrium provides a prototype example of a transient interaction. Here, the wave has generally a modest influence on the background structure of the atmosphere. The convective activity, however, responds to the vertical motions associated with the wave. In effect, the convection modifies the environment through which the wave propagates. Essentially, this interaction damps the wave and causes the disturbance to sense a reduced

* Corresponding author: Department of Meteorology, University of Stockholm, S-106 91 Stockholm, Sweden.

static stability (Emanuel *et al.* 1994). Radiative heat transfer acts in most circumstances to damp wave motions as well, but the time-scale of this process generally exceeds that of the convective damping.

Stationary interactions between flows and the environment, on the other hand, may result in a new background state which differs significantly from a locally determined radiative–convective equilibrium. Here, the effect of the clear-sky water vapour and clouds on atmospheric radiation plays an instrumental role in reshaping the environment. Still, the primary interaction can be thought to occur between the flow and the convection, which in turn alters the distribution of infrared absorbers. An interesting study by Held *et al.* (1993) illustrates the potential of large-scale circulations to alter their environment. In a two-dimensional radiative–convective model with explicit moist convection, they obtain one equilibrium where the convection, on average, occurs homogeneously, and one equilibrium where the convection is localized within a small part of the domain. The latter equilibrium is associated with a large-scale circulation that descends in the bulk of the domain.

This work emphasizes stationary interactions between atmospheric flows and their environment. We focus on the case where the forcing (primarily the insolation) is identical in the two columns. This implies that local radiative–convective equilibrium, in which the two columns are identical, is a stationary solution. A central, and by no means trivial, question is if, and under which conditions, the two-column radiative–convective model may attain equilibria with a large-scale circulation.

To illuminate the physics involved, consider an inviscid two-column system, initially at rest, in which one column is a few degrees cooler than the temperature determined by local radiative–convective equilibrium. (Effects of the oceanic response time and wind-induced heat exchange (Emanuel 1987; Neelin *et al.* 1987) can be suppressed if we tactically assume an oceanic mixed layer with negligible heat capacity.) Obviously, the cold anomalous column is relaxed towards the local equilibrium by reduced emission of infrared radiation. In addition, the initial temperature contrast produces a circulation with descent in the cold column. Even in strongly convecting atmospheres, large-scale motions sense a positive, effective static stability (e.g. Neelin and Held 1987; Emanuel *et al.* 1994; Yu *et al.* 1998). Therefore, the cold column is warmed by subsidence while the updraught column is cooled. If no further process operates, the result would be essentially an internal gravity wave that is damped by radiative–convective processes. Eventually, the local equilibrium is re-established.

Consider next how interaction between the flow and the infrared radiation—mediated by the clear-sky distribution of water vapour—may maintain or amplify the disturbance. Most transparently, the mechanism appears if we think of the limiting case of zero effective static stability, in which the flow no longer produces any advective temperature tendencies. Still, the decline of specific humidity with height causes any flow to modify the distribution of water vapour. Let us consider the effects of a flow in the inviscid two-column system, which now is assumed, initially, to have horizontally homogeneous temperature and humidity. The flow acts to moisten the updraught column and to dry the downdraught column. As the opacity of the atmosphere to terrestrial radiation increases with the humidity, the emission of infrared radiation is enhanced from the latter column while it is reduced in the former. Thereby, a column temperature contrast is created that accelerates the flow. The effective emissivity of the system is increased generally by the flow: the drying of the downdraught column (where the moisture tendencies of advection and convection are opposite) is more pronounced than the moistening of the updraught column. Therefore, the system drifts from the local radiative–convective equilibrium to a cooler climate with a steady, large-scale circulation.

Pierrehumbert (1995) argues that the potential of large-scale circulations to create dry-air pools in regions of subsidence is instrumental in determining the sensitivity of the tropical climate; he called the dry emissive pools 'radiator fins'. In the picture of Pierrehumbert, the dryness and the horizontal extent of the radiator fin are the key determinants of the tropical climate. Our work connects to ideas of Pierrehumbert (1995) as we here consider the conditions under which a radiative–convective two-column model may attain equilibrium with a large-scale circulation. In the present model, however, we keep the horizontal areas of the two columns equal.

It is important to remember that we use clear-sky conditions in the radiation calculation. To the lowest order, however, we believe that clouds act essentially to re-enforce the effects on the radiation budget that results from the interaction between clear-sky water vapour and large-scale flows. In the descending branch, advective drying and the formation of low, extensive cloud decks with high albedo have, qualitatively, a similar effect on the net radiative cooling of the column (e.g. Miller 1997); and observations in the Tropics indicate that deep clouds—concentrated in the ascending branch of the circulation—have little effect on the net radiation at the top of the atmosphere (Ramanathan *et al.* 1989; Pierrehumbert 1995). In any event, this study may be instructive in showing what aspects of large-scale steady atmospheric circulations that can be reproduced by our model, in the absence of cloud–radiation feedback.

This paper is organized as follows: the model is briefly described in section 2; a conceptual model of circulations with two-column structure that interact with radiative–convective processes is discussed in section 3; in section 4, the model results are presented; and in section 5, we address some questions which the present study has left open.

2. Model description

The present side-by-side two-column model is an extension of the single-column model for radiative–convective equilibria described by Rennó *et al.* (1994a). Figure 1 delineates the structure of the model. The model is formulated in pressure coordinates with 30 levels in the vertical. In the finite-difference formulation, an upwind scheme is used for the advective terms. The time integration is performed by a leapfrog scheme with an Asselin filter applied (Asselin 1972). The governing equations are summarized below.

The tendencies of temperature, T, and specific humidity, q, are computed as

$$c_p \frac{\mathrm{D}T}{\mathrm{D}t} - \rho^{-1}\omega = Q, \tag{1}$$

$$\frac{\mathrm{D}q}{\mathrm{D}t} = C, \tag{2}$$

where the rate of change following a fluid element (moving with the velocity (u, ω)) is defined by

$$\frac{\mathrm{D}}{\mathrm{D}t} \equiv \frac{\partial}{\partial t} + u\frac{\partial}{\partial x} + \omega\frac{\partial}{\partial p}. \tag{3}$$

Here, p is pressure, c_p and ρ are the heat capacity at constant pressure and the density of air, respectively, Q is the heating rate per unit mass, which comprises a radiative and a convective part as well as surface fluxes, and C is the moisture source due to convection and evaporation from the surface. The radiative heating is computed by the radiation

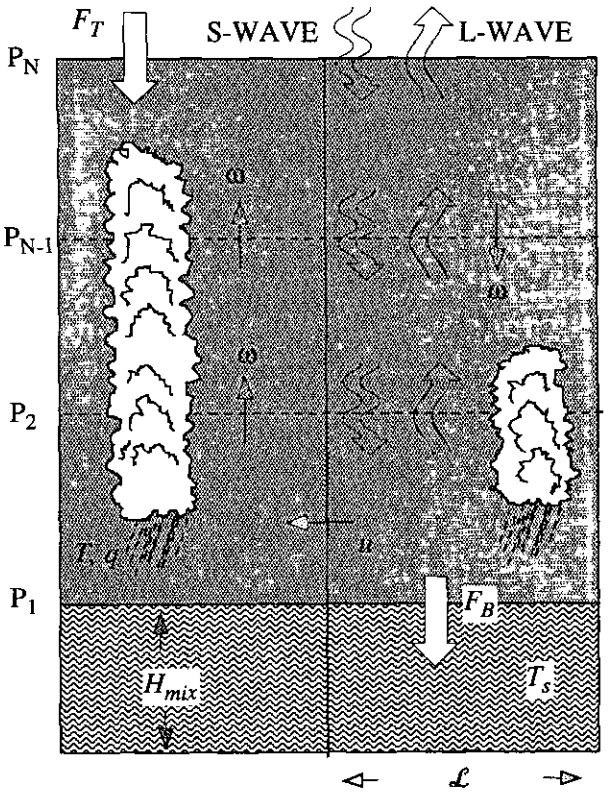

Figure 1. Schematic of the structure of the two-column model. At each of the 30 vertical levels, the temperature T and specific humidity q are calculated. The scheme of Emanuel (1991) gives the convective tendencies and a radiation parametrization by Chou *et al.* (1991) and Chou (1992) calculates the short- and long-wave radiation using clear-sky conditions. A flow field (u, ω), predicted by the linear, hydrostatic equations of motion in a non-rotating frame of reference, produces advective tendencies in the heat and moisture budgets. An ocean mixed layer, of temperature T_s, exchanges heat and moisture with the atmosphere. The net vertical heat fluxes at the top and bottom of the atmosphere are denoted F_T and F_B, respectively, and $\mathcal{L}$ is the column length.

parametrization developed by Chou *et al.* (1991) and Chou (1992). Clear-sky conditions are assumed in the radiation calculation. The convection is represented by the Emanuel scheme (we use the version 2.03; for details see Emanuel (1991)). Further details of the radiative–convective code are described by Rennó *et al.* (1994a,b).

A bulk formula is used to compute the upward fluxes of sensible and latent heat at the sea surface:

$$F^S = \rho_a C_E V_a (T_s - T_a) c_p, \tag{4a}$$

$$F^L = \rho_a C_E V_a (q_s - q_a) L_v, \tag{4b}$$

where the subscripts a and s refer to properties of the near-surface air and to the sea surface, respectively, C_E is an exchange coefficient, V_a is the near-surface wind speed (assigned a fixed value), and L_v is the latent heat of vaporization. As customary, q_s is assumed to have the saturation value at the sea surface temperature T_s. No explicit diffusion of heat or moisture is represented in the model, and therefore the fluxes of sensible heat and moisture across the sea surface are distributed evenly over the lowest model level.

Dynamically, the system is linear, hydrostatic and non-rotating; the governing equations are

$$\frac{\partial u}{\partial t} = -\frac{\partial \Phi}{\partial x} + \mu \frac{\partial^2 u}{\partial p^2}, \tag{5a}$$

$$\frac{\partial \Phi}{\partial p} = -\rho^{-1}. \tag{5b}$$

Here, μ represents the viscous damping and Φ is the geopotential height. The density of air is computed from the gas law (e.g. Emanuel 1994)

$$\rho^{-1} = \frac{R_d(1 - q + q/\epsilon)T}{p}, \tag{6}$$

where R_d is the gas constant for dry air and ϵ is the ratio between the molecular masses of water vapour and of dry air. At the surface, the boundary condition for the horizontal velocity is a linearized surface-drag formula

$$-g^{-1}\mu \frac{\partial u}{\partial p} = \rho_a C_D V_a u, \tag{7a}$$

where g is the acceleration of gravity and C_D the surface drag coefficient. A free-slip boundary condition is applied at the top of the atmosphere, which requires that

$$\frac{\partial u}{\partial p} = 0. \tag{7b}$$

The continuity equation

$$\frac{\partial u}{\partial x} + \frac{\partial \omega}{\partial p} = 0, \tag{8a}$$

allows the velocity field to be expressed in terms of a stream function, Ψ:

$$(u, \omega) = \left(-g\frac{\partial \Psi}{\partial p}, g\frac{\partial \Psi}{\partial x}\right). \tag{8b}$$

In our two-column formulation, where the two columns are of equal length, we use the convention that the updraught column (distinguished by the subscript 1) is located to the left and the downdraught column (distinguished by the subscript 2) is located to the right. Thus, the vertical velocities, in the updraught and the downdraught column, are given by

$$\omega_1 = g\mathcal{L}^{-1}\Psi(p, t), \quad \omega_2 = -g\mathcal{L}^{-1}\Psi(p, t), \tag{9}$$

respectively, where $\mathcal{L}$ is the column length.

The model atmosphere is situated above an ocean mixed layer, whose temperature is governed by

$$\rho_s c_{p_s} H_{mix} \frac{\partial T_s}{\partial t} = -F_B, \tag{10}$$

where ρ_s and c_{p_s} are the density and the heat capacity of sea water, respectively, and H_{mix} is the mixed-layer depth. The net, upward heat flux at the sea surface F_B is comprised of sensible- and latent-heat flux components (given by Eqs. (4a) and (4b)) and a radiative-heat flux, which includes solar and infrared atmospheric radiation as well as black-body radiation from the sea surface.

3. A CONCEPTUAL MODEL OF CIRCULATIONS WITH TWO-COLUMN STRUCTURE

Before presenting the results of the present model, we discuss the physical features of atmospheric circulation patterns that have a two-column structure. Here, one column (the updraught column) represents the ascending branch of a large-scale circulation pattern, and the other (the downdraught column) represents the descending branch of the circulation. To narrow the scope of this section, we focus on the case where the solar forcing and the horizontal extent of the two columns are equal.

(a) *The moist static energy budget*

The dry and moist static energies are defined as (e.g. Emanuel 1994)

$$h_d \equiv c_p T + \Phi, \quad h \equiv h_d + L_v q. \tag{11}$$

If transport of kinetic energy is neglected, which is a good approximation for the present consideration, the rate of change of moist static energy is governed by (e.g. Neelin and Held 1987)

$$\frac{\partial h}{\partial t} = -\nabla \cdot (h\mathbf{u}) + g\frac{\partial F}{\partial p}. \tag{12}$$

where $F = F^R + F^S + F^L$ is the net vertical heat flux, which is comprised of a radiative-, a sensible-, and a latent-heat flux component. At the top of the convective layer, F is purely radiative.

By taking the horizontal average of the vertically integrated moist static energy equation over the updraught and downdraught columns, respectively, we get

$$\left\langle \left(\frac{\partial h}{\partial t}\right)_1 \right\rangle = -\langle \nabla \cdot (h\mathbf{u})_1 \rangle + F_{B1} - F_{T1}, \tag{13a}$$

$$\left\langle \left(\frac{\partial h}{\partial t}\right)_2 \right\rangle = -\langle \nabla \cdot (h\mathbf{u})_2 \rangle + F_{B2} - F_{T2}. \tag{13b}$$

Here the subscripts 1 and 2 refer to the updraught and downdraught column, respectively, F_B and F_T are the net upward heat fluxes at the sea surface and the top of the atmosphere, respectively; and the column average, for an arbitrary quantity a, is defined through

$$\langle a \rangle \equiv \frac{1}{g\mathcal{L}} \iint a \, \mathrm{d}x \, \mathrm{d}p.$$

Motivated by observations (Neelin and Held 1987), we assume that the divergence of the flow has a simple structure, with one sign near the sea surface and the opposite sign in the upper troposphere. We let the values of the moist static energy in the lower and upper troposphere be represented by h_b (the subcloud-layer moist static energy) and $h_b + \Delta h_0$, respectively, where Δh_0 is the difference in moist static energy between the upper and lower troposphere; note that this quantity is essentially the gross moist stability as defined by Neelin and Held (1987). Using this notation, we approximate the advective tendencies in the updraught column as

$$-\langle \nabla \cdot (h\mathbf{u})_1 \rangle \approx -\omega_+ (\Delta h_b + \Delta h_0) \, g^{-1}, \tag{14a}$$

and in the downdraught column as

$$-\langle\nabla\cdot(h\mathbf{u})_2\rangle\approx+\omega_+\,(\Delta h_b+\Delta h_0)\,g^{-1}. \tag{14b}$$

Here, ω_+ is the magnitude of the pressure velocity just above the subcloud layer, and $\Delta h_b\equiv h_{b1}-h_{b2}$ is the column difference in moist static energy of the subcloud layer.

Neelin and Yu (*1994*) and Yu and Neelin (*1997*) analyse the interplay between large-scale dynamics and convection in continuously stratified atmospheres. They show that a constraint on the convection to be in quasi-equilibrium with the dynamics singles out a deep-convective mode. This mode has a well-defined gross moist stability and its dispersion properties turn out to be mathematically identical to those of the two-level description. Using soundings of the background stratification, Yu *et al.* (1998) produce maps of the gross moist stability in the Tropics.

To close the Eqs. (14a) and (14b), we make the questionable but simplifying assumption that the relative humidity of the subcloud layer is constant. In this case, Δh_b can be phrased in terms of the column difference in near-surface air temperature (ΔT_a) according to

$$\Delta h_b=ac_p\Delta T_a, \tag{15}$$

where a is approximately given by

$$a=1+\frac{RH\,L_v}{c_p}\left(\frac{\partial q^*}{\partial T}\right)_{T_a}.$$

Here, RH is the relative humidity and q^* is the specific humidity at saturation.

(*b*) *The vertical heat flux*

As a reference state, we assume a radiative–convective equilibrium. Thus, in the reference state we have

$$F_B-F_T=0.$$

The flux of radiation at the top of the atmosphere depends on the details of the vertical distribution of temperature and moisture in the column. To extract, in its simplest form, the physics involved in destabilizing the local radiative–convective equilibrium, it is sufficient to approximate F_T as a function of the near-surface air temperature and the vertical velocity. Basically, the argument is that the large-scale vertical motion acts to dry the downdraught column and moisten the updraught column. As water vapour is the major infrared absorber, the humidity of the column determines essentially the opacity to the upwelling terrestrial radiation. Evidently, vertical motions do not change the moisture distribution instantly; there is a finite response time. However, as we emphasise the steady states of the system, we may ignore the details of the transient response.

By taking the radiative–convective equilibrium as a reference state, we parametrize the anomaly in radiative flux at the top of the atmosphere as

$$F_T'=(T_a-T_e)\left(\frac{\partial F_T}{\partial T_a}\right)+\omega_+\left(\frac{\partial F_T}{\partial\omega_+}\right), \tag{16}$$

where T_e is the surface air temperature in the reference state. In essence, this linearized formula approximates the dependence of the outgoing infrared radiation on the temperature and the optical thickness of water vapour in the column. Note that F_T tends to increase with descending motion, which dries the atmosphere. To the extent that the

distribution of clouds is related to the large-scale vertical velocity, cloud–radiative feedback could also be incorporated, crudely, in the second term on the right-hand side of Eq. (16). Qualitative support for the present parametrization of F_T is given by Sherwood (1996), who finds a high correlation between outgoing long-wave radiation and large-scale vertical motion in the Tropics.

It is clarifying to point out an assumption inherent in Eq. (16): deep convection is the agent that couples the local surface air temperature, via communication with the subcloud layer, to the atmospheric temperature structure aloft. In regions of strong subsiding motion, a trade inversion may form that disconnects the subcloud layer and, therefore, the surface temperature from the temperature of the free atmosphere. When an inversion forms, the relation in Eq. (16) has to be modified.

Next, we consider the heat flux at the sea surface. To keep our conceptual model transparent, we neglect any influence on the atmospheric dynamics that may be related to the thermal inertia of the oceanic mixed layer. Instead, we focus on two instructive limiting cases: mixed layers of zero and of infinite heat capacity, respectively. For zero oceanic heat capacity, F_B vanishes. Here, the sea surface temperature (SST) instantaneously adjusts to the value which yields zero heat flux. An infinite oceanic heat capacity, on the other hand, is equivalent to a fixed SST. In this case, the humidity and temperature of the near-surface air essentially determine F_B.

For atmospheric phenomena with short time-scales (of the order of days), a fixed SST may serve as suitable idealization of the lower thermodynamic boundary condition. When the mean state or low-frequency phenomena are addressed in an atmospheric model coupled to an oceanic mixed layer, a boundary condition of zero heat flux at the sea surface is a more relevant approximation (Seager *et al.* 1995; Marotzke and Pierce 1997).

To approximate the surface heat flux in a situation with fixed SST, we once more take the radiative–convective equilibrium as a reference state. For simplicity, we ignore changes in the radiative flux at the surface, which are usually small compared to the changes in the latent- and sensible-heat fluxes. As we have assumed a constant relative humidity, we can phrase the heat-flux anomaly as

$$F'_B = (T_a - T_e)\left(\frac{\partial F_B}{\partial T_a}\right)_{RH,\,T_e}, \tag{17a}$$

where

$$-\left(\frac{\partial F_B}{\partial T_a}\right)_{RH,\,T_e} \equiv \lambda \approx \rho_a C_E V_a c_p a. \tag{17b}$$

In the Tropics, λ is typically of the order of 40 W m^{-2} K^{-1} (Gill 1982). As a consequence of the high sensitivity of the sea surface heat flux with temperature, the near-surface air temperature and the SST are nearly identical over the tropical oceans (e.g. Pierrehumbert 1995).

(*c*) *The atmospheric circulation*

We use a simple, linear relation between the distribution of near-surface air temperature and the pressure velocity at the top of the subcloud layer, which in the two-column (finite-difference) formulation takes the form

$$t_d \frac{\partial \omega_+}{\partial t} = \gamma \Delta T_a - \omega_+. \tag{18a}$$

Here, t_d is the mechanical-damping time-scale and it is estimated as

$$\frac{1}{t_d} = \frac{g\rho_a V_a C_D}{p_0} + \frac{\mu}{{p_0}^2}, \tag{18b}$$

where p_0 represents the pressure thickness of the subcloud layer. In Eq. (18b), the first term on the right-hand side stems from drag at the sea surface and the second term from drag at the top of the subcloud layer. In the limiting case of a nearly inviscid atmosphere, the former drag contribution dominates. The parameter γ, which measures the flow intensity per unit temperature difference, is defined as

$$\gamma \equiv \frac{t_d \varphi}{\mathcal{L}^2}, \tag{18c}$$

where φ depends on the details of the flow. Depending on the intensity of the circulation, two different lines of argument can be used to estimate φ, with similar but slightly different results; see Neelin (1989) and Yu and Neelin (1997) for a discussion.

For flows weak compared to the radiatively forced subsidence in clear skies, it can be assumed that convection communicates the subcloud distribution of moist static energy throughout the convecting layer, which is forced to have an essentially moist adiabatic lapse rate. For this case, Emanuel *et al.* (1994) show how the vertical motion, in a non-rotating system, can be calculated from curvature of the distribution of subcloud, moist static energy (here assumed to be proportional to ΔT_a; see Eq. (15)). A more elaborate treatment is given by Neelin and Yu (1994) and by Yu and Neelin (1997).

Stronger flows, however, may create a trade inversion which disconnects the near-surface air from the free atmosphere. For such flows, Lindzen and Nigam (1987) give a physical discussion of how the low-level flow field can be deduced from the distribution of the surface temperature. Note that they use the SST distribution in their diagnostic calculations; the tight coupling between the SST and the near-surface air temperature makes this an excellent approximation.

Our primary use of the flow law Eq. (18a) is to scale the equations and identify non-dimensional parameters. To this end, the precise value of φ is of no vital importance. Here, we use a form that can be deduced from the arguments of Lindzen and Nigam (1987):

$$\varphi = \frac{{p_0}^2 R_d}{2p_s}, \tag{18d}$$

where p_s is the surface air pressure.

(*d*) *Stability of the local equilibrium and non-dimensional parameters*

We now return to the column budgets of moist static energy. By taking the difference between Eq. (13a) and Eq. (13b) and using the approximate relations derived above, we get

$$\left\langle \left(\frac{\partial h}{\partial t}\right)_1 - \left(\frac{\partial h}{\partial t}\right)_2 \right\rangle = -2\omega_+(ac_p\Delta T_a + \Delta h_0)g^{-1} + \Delta F_1 - \Delta F_2, \tag{19}$$

where $\Delta F_{1/2} \equiv F_{B1/2} - F_{T1/2}$. When the heat flux vanishes at the sea surface (i.e. $F_B = 0$), we have (see Eq. (16))

$$\Delta F_1 - \Delta F_2 = -\beta \Delta T_a + 2\omega_+ \sigma g^{-1}. \tag{20a}$$

A prescribed SST, on the other hand, yields (see Eq. (17a))

$$\Delta F_1 - \Delta F_2 = -(\beta + \lambda)\Delta T_a + 2\omega_+ \sigma g^{-1}. \tag{20b}$$

Here, we have introduced

$$\beta \equiv \left(\frac{\partial F_T}{\partial T_a}\right), \quad \sigma \equiv \frac{g}{2}\left\{\left(\frac{\partial F_T}{\partial \omega_+}\right)_2 - \left(\frac{\partial F_T}{\partial \omega_+}\right)_1\right\}.$$

For the sake of generality, we will use Eq. (20b) in the rest of this section. The case with zero heat flux at the sea surface is recovered simply by setting λ to zero.

On the right-hand side of Eq. (20b), the two first terms represent restoring effects due to the temperature dependence of the infrared radiation and the surface heat exchange, while the last term represents a destabilizing effect of the infrared radiation due to advective drying and moistening. (Note that it is possible to include additional feedbacks between the circulation and the radiation in the definition of σ. For example, we may use the definition $\sigma = \sigma_V + \sigma_C$; where σ_V and σ_C are related to the clear-sky water vapour and the distribution of clouds, respectively.)

To assess, qualitatively, the stability of the local equilibrium to large-scale flows, we evaluate the derivative of Eq. (19) with respect to ω_+. By assuming a balanced flow (i.e. using the steady-state version of the flow law Eq. (18a)), we arrive at

$$g\frac{\partial}{\partial \omega_+}\left\langle\left(\frac{\partial h}{\partial t}\right)_1 - \left(\frac{\partial h}{\partial t}\right)_2\right\rangle_{\Delta T_a = 0} = -2(\Delta h_0 - \sigma) - \frac{g(\beta + \lambda)}{\gamma}. \tag{21}$$

The sign of this expression indicates whether the local radiative–convective balance may be destabilized and yield an equilibrium with large-scale circulation. We emphasise that Eq. (21) does not provide a strict criterion of stability as we have ignored the response times of the circulation and the advective drying. Rather, the relation Eq. (21) provides a rough indication of the character of the steady states: when it is positive, we expect that equilibria with a large-scale overturning circulation are attainable; and when Eq. (21) is negative, we expect to find the system in radiative–convective equilibrium.

It is instructive to consider the stability features in the limiting case of an inviscid atmosphere. Here, the temperature dependence of the infrared radiation and the surface heat flux gives no stabilizing effect as the column-temperature contrast vanishes in the presence of a steady flow (see the definition of γ in Eq. (18c)). The local equilibrium is stable in the inviscid limit provided that the gross moist stability (Δh_0) is larger than σ, which measures the positive feedback between radiation and circulation. In line with Neelin and Held (1987), it seems appropriate to call the term $\Delta h_0 - \sigma$ (which may be negative) the gross moist-radiative stability.

A convenient measure of the ability of the flow to destabilize the local equilibrium is provided by the following non-dimensional parameter:

$$\Gamma \equiv \frac{2\gamma(\sigma - \Delta h_0)}{g(\beta + \lambda)}. \tag{22}$$

As defined here, the local equilibrium is stable when Γ is less than unity. Typical values of β and λ are 2 W m^{-2} and 40 W m^{-2}, respectively. Thus, it is evident that a prescribed SST has a strong stabilizing effect on the system. Note that Γ approaches infinity as the mechanical damping (or the column length) goes to zero. In what follows, we will refer to Γ as the flow parameter.

We note that in this model, the local equilibrium becomes increasingly unstable for shrinking column length. In nature, horizontal eddy moisture transport (which may be represented as diffusion) into the region of subsidence would presumably limit the smallest scale of steady circulation patterns.

(e) *Further aspects of the conceptual model*

In this model, the nonlinearity of the advective tendency, related to the difference in subcloud-layer moist static energy, limits eventually the destabilizing tendency due to advective drying. Solving for the surface temperature difference in the steady state (Eq. (19) together with Eq. (18a)), we find, in addition to the radiative–convective equilibria ($\Delta T_a = 0$), a time-independent solution with circulation and a temperature contrast given by

$$\Delta T_a = \frac{2\gamma(\sigma - \Delta h_0) - g(\beta + \lambda)}{2c_p a\gamma} = \frac{(\sigma - \Delta h_0)}{c_p a}\left(1 - \frac{1}{\Gamma}\right), \tag{23}$$

provided that Γ is larger than unity. This relation may approximate the SST difference for weak flows, which only moderately modify the radiative–convective equilibria. For vigorous flows, however, we expect that this formula, which relies on a linearization with respect to the local equilibrium, loses its predictive value.

The relation Eq. (23) predicts that ΔT_a saturates for large Γ. The vertical velocity, on the other hand, is predicted to increase linearly with the flow parameter according to

$$\omega_+ = \frac{g(\beta + \lambda)}{2c_p a}(\Gamma - 1). \tag{24}$$

However, the local heat-balance (Eq. (1)) (or the column budget of dry, static energy) imposes an upper limit on the vertical velocity in regions of subsidence. In the middle troposphere, the diabatic cooling, which balances the adiabatic heating of the subsiding air, is limited above by the radiative cooling in clear skies ($\dot{Q}_{\text{rad}}$): that is,

$$\omega \frac{\partial}{\partial p}(c_p T + \Phi) \approx \dot{Q}_{\text{rad}}.$$

As a first approximation, we suppose that the large-scale circulation has only a moderate influence on the clear-sky radiative cooling rate and the lapse rate in the system. The maximum vertical velocity, then, is set by the clear-sky subsidence rate in local radiative–convective equilibrium; and accordingly the vertical velocity scales as

$$\omega_{\text{rad}} = \dot{Q}_{\text{rad}} \left(\frac{\partial h_d}{\partial p}\right)^{-1}. \tag{25}$$

where $(\partial h_d/\partial p)$ is the vertical gradient of dry static energy.

Returning to the Eq. (24), we find that the value of Γ that yields ω_{rad}, say Γ_{rad}, is

$$\Gamma_{\text{rad}} = \frac{\omega_{\text{rad}} 2c_p a}{g(\beta + \lambda)} + 1. \tag{26}$$

Based on our simplified, conceptual discussion of the two-column system, we can delineate crudely the evolution of the equilibria as the flow parameter increases. For Γ-values less than unity, we anticipate the system to be in radiative–convective equilibrium. As Γ is increased above unity (by reducing the viscosity or the horizontal length-scale) the system will be in an equilibrium with a large-scale circulation. As Γ becomes comparable to Γ_{rad}, or larger, the flow intensity will be controlled by thermal processes rather than by frictional resistance. In this regime, we expect that the subcloud layer in the downdraught column disconnects gradually from the free atmosphere and that a mechanical boundary layer begins to form near the surface. Here, the interior

atmosphere approaches an inviscid state. Further increase of Γ affects primarily the height and velocity of the viscous boundary layer.

To be sure, this crude, conceptual model fails to capture the full complexity of the real atmosphere or, for that matter, the present numerical model. Nevertheless, one aspect that we anticipate to be robust is that the mechanical damping and the length of the domain affect the equilibrium states only through the non-dimensional parameter Γ. In addition, we expect that the equilibria of the model become essentially independent of Γ provided that it is much larger than Γ_{rad}.

4. EQUILIBRIUM STATES OF THE TWO-COLUMN MODEL

Here, we delineate salient features of the equilibrium states of the two-column model. We emphasise that, in the present model integrations, all external parameters (e.g. the solar forcing and the parameters in the convective scheme) are identical in the two columns. Consequently, local radiative equilibrium is a steady, but not necessarily stable, solution. The single-column equilibrium states of the present radiative–convective code have been investigated thoroughly by Rennó (1997) and by Rennó *et al.* (1994a,b).

The model is forced with the annually averaged insolation at 30° latitude (373 W m^{-2}), which for (single-column) radiative–convective equilibrium gives an SST of 38°C. To some extent, our choice of solar forcing is arbitrary. But as we demonstrate, the large-scale circulation significantly cools the climate. One motive, however, for choosing a reference state which is quite warm is that the potential effect of advective drying on the radiative fluxes increase with temperature. (This applies, to be accurate, to a reference state with a fixed profile of relative humidity.) Some of the physical parameters are listed in Table 1.

In addition to the local radiative–convective equilibrium, the two-column model may have steady, circulating equilibria with ascent in one column and descent in the other. We focus on how the steady-state solutions depend on the additional physical parameters that are introduced in the two-column model. These parameters are the column length ($\mathcal{L}$), the viscous damping (μ), and the surface drag coefficient (C_D). As advocated in section 3 and verified later, the magnitude of these parameters affects the steady, equilibrium states only via the non-dimensional parameter Γ (the flow parameter, see

TABLE 1. PARAMETERS

Parameter	Value	Units
Solar constant	1382.00	W m^{-2}
Surface albedo	0.1	—
Amount of CO_2	330.00	ppm
Model latitude	30.0	degrees
Column length, $\mathcal{L}$	3 to 300	degrees
Surface wind speed, V_a	7.0	m s^{-1}
Viscosity, μ	variable	kg^{2}m^{-2}s^{-3}
Drag coefficient, C_D	variable	—
Exchange coefficient, C_E	10^{-3}	—
Mixed-layer depth, H_{mix}	5.0	m
PB_{crit} (†)	100.00	mb
PT_{crit} (†)	400.00	mb
σ_d (†)	0.04	—
σ_s (†)	0.15	—

(†) Cloud microphysical parameter of the Emanuel scheme.

Eq. (22)). An important aim is to investigate how the flow parameter influences the equilibrium states. In this endeavour, we keep all parameters fixed, except for the column length and mechanical damping, which are varied to produce different Γ-values.

To quantify the flow parameter Γ (as we vary $\mathcal{L}$, μ, and C_D), we need to estimate some physical parameters (see Eqs. (22) and (18c)). Based on the results of the present model, a crude estimate gives

$$p_0 \approx 135 \text{ mb}, \quad \beta \approx 2 \text{ W m}^{-2}\text{K}^{-1}, \quad \frac{\sigma - 2\Delta h_0}{c_p} \approx 2 \text{ K}, \quad a \approx 4.$$

And an estimate of Γ_{rad} (using $\omega_{\text{rad}} = 20 \text{ mb d}^{-1}$) yields

$$\Gamma_{\text{rad}} \approx 10.$$

It is worth stressing that the exact values of these parameters are not vital when we stratify the equilibria of the model according to Γ. If some parameter is erroneous, the main effect is that the transition from local to circulating equilibria no longer occurs when the flow parameter is near unity. Here, the crucial issue is that Γ is proportional to the mechanical-damping time-scale and inversely proportional to the square of the column length.

(a) *The general features of equilibrium states of the two-column model*

To study the limit of weak, mechanical damping, we consider initially a situation with zero surface drag. In this set of calculations, we initialize the system with identical atmospheric soundings (taken from the radiative–convective equilibria), but with a difference in SST between the two columns of a few degrees Kelvin. The integration of the model is continued until it reaches a steady state. All equilibria presented here, and this we emphasize, are found by integration of a time-dependent model.

Figures 2(a) and (b) show the equilibrium SST in the downdraught column and column difference in SST, respectively, as functions of the parameter Γ. Note that the SST closely reflects the surface air temperature in the model. It is illuminating to think that these graphs portray the evolution of the equilibria as the flow parameter is increased (by reducing the mechanical damping or the column length) slowly enough to keep the system in a quasi-steady state. The steady-state difference in SST reveals the broad character of the equilibrium state as it reflects roughly the intensity of the large-scale circulation. Generally, the equilibrium state gets colder and develops a more intense circulation as the flow parameter increases. The parameter space is characterized by two main bifurcations.

The first bifurcation occurs near $\Gamma = 2$; and it is associated with the transition from local radiative–convective equilibria to equilibria with a large-scale overturning circulation. This first bifurcation is supercritical, as the difference in SST and the intensity of the circulation increase continuously from zero as Γ surpasses the critical value. The influence of Γ on the equilibrium SST saturates gradually; it becomes nearly insignificant somewhere beyond $\Gamma = 50$. At that stage, the mid-troposphere vertical velocity has essentially reached the radiatively determined limit ω_{rad} (see Fig. 4), and the vertically integrated convective heating is small in the downdraught column. The interior atmosphere is now nearly inviscid and a mechanical boundary layer begins to appear. Further increase in the flow parameter affects mainly the thickness and velocity of the mechanical boundary layer.

A second, subcritical bifurcation occurs near $\Gamma = 200$. Here, a second type of equilibrium becomes attainable that is colder and has stronger near-surface circulation.

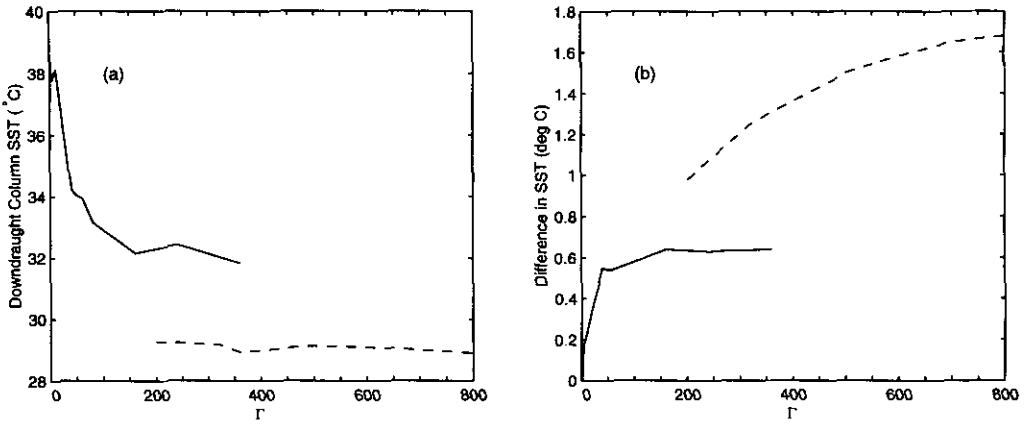

Figure 2. (a) The equilibrium sea surface temperature (SST) of the downdraught column, and (b) the equilibrium column difference in SST, as functions of the non-dimensional parameter Γ (see text), which is proportional to the mechanical-damping time-scale and inversely proportional to the square of the column length. The two-column model has two equilibria with large-scale circulation: one with deep convection in the downdraught column (the solid line), and one for which the subcloud layer is decoupled from the free atmosphere in the downdraught column, where convection is absent (the dashed line). For values of Γ less than unity, local radiative–convective equilibrium is the only stationary solution.

In the new equilibrium, the near-surface boundary layer in the downdraught column is disconnected, by an inversion, from the atmosphere aloft, and convection has ceased entirely in that column (see Fig. 3). The Emanuel scheme, which we use, is capable of representing shallow convection (Emanuel 1991). In the regime where the second equilibrium state appears, however, the thickness of the mechanical boundary layer strongly controls the height of the inversion, and thereby the height of any shallow, convective activity. For the present parameter configuration, the mechanical boundary layer is thin enough to suppress convection entirely. In any event, the most crucial feature of the second type of equilibrium is that the convective activity has ceased above the inversion, which yields a dry atmosphere that is more transparent to infrared radiation; and whether or not shallow convection occurs below the inversion is likely to have a weak influence on the infrared radiation that escapes from the top of the column—at least if the interaction between clouds and radiation is ignored as in the present radiation calculation.

In a limited regime, the system has two distinct equilibria with circulation. Here, the initial conditions determine which equilibria the system attains. A strong initial temperature contrast favours the solution with shallow (or no) convection. For Γ-values exceeding approximately 400, the solution with deep convection in the descent column becomes unstable and is no longer attainable in our time-dependent integration. Somewhere beyond $\Gamma = 1400$, we no longer find steady equilibria. Here, the second solution begins to exhibit temporal oscillations around its mean state. In the present work, we do not further explore the oscillatory regime. It is interesting to note that Rennó (1997) also finds multiple equilibrium states in a single-column model using, essentially, the present radiative–convective code. We believe that the phenomenon of multiple equilibria is a physical feature of moist atmospheric models that transcends the particular choice of radiative–convective parametrization. In essence, these multiple equilibria reflect the large degree of freedom of the water-vapour distribution in the model atmospheres. It is a different issue, however, if multiple equilibria exist in nature or may occur also in models of moist atmospheres with higher horizontal resolution.

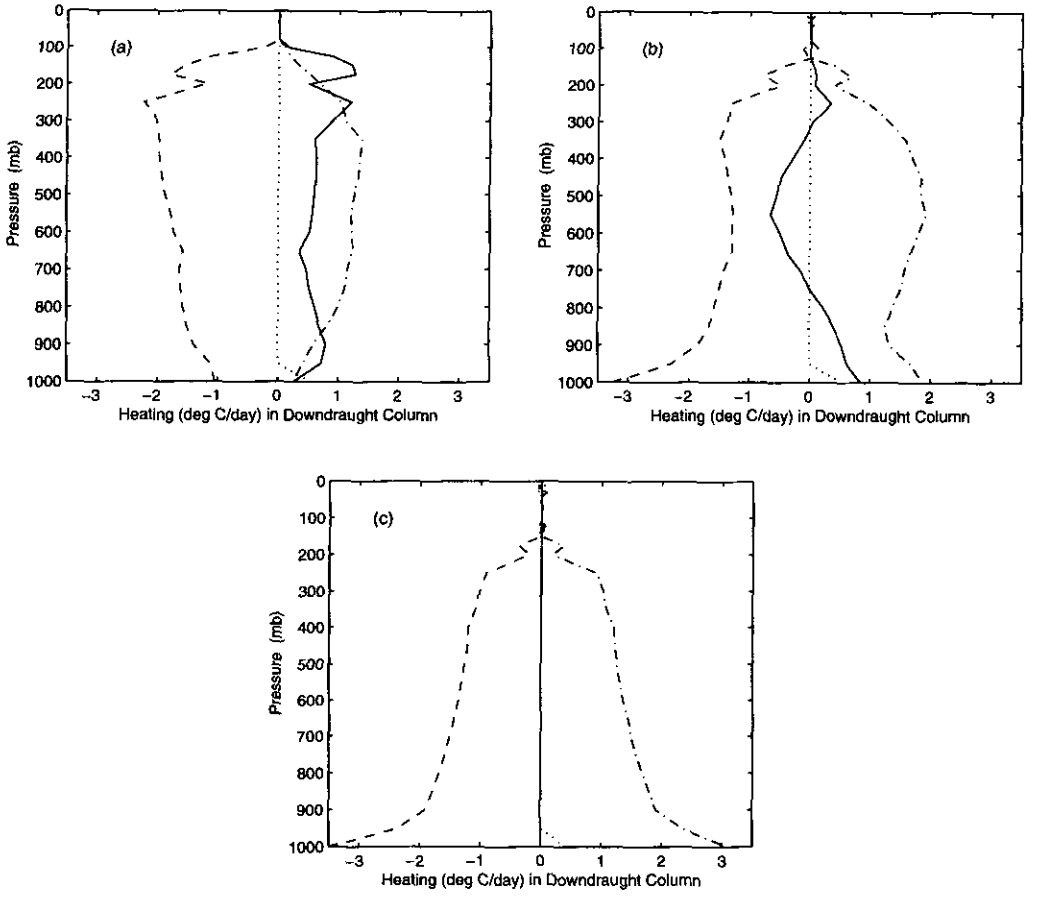

Figure 3. Downdraught-column profiles of heating by convection (solid line), radiation (dashed line), advection (dash-dotted), and surface fluxes (dotted). Three different flow regimes are portrayed: (a) moderately perturbed radiative–convective equilibrium at flow parameter $\Gamma = 4$; (b)–(c) strongly perturbed radiative–convective equilibrium at $\Gamma = 360$, where the system has one equilibrium with deep convection (b) and one without convection (c). Deep convection is always present in the updraught column.

Besides providing enhanced mechanical damping, surface drag in the model produces no significant modifications of the features of the equilibria. Gradually increasing the surface drag (which reduces the flow parameter, see Eq. (18b)) essentially causes the steady state to trace backwards the equilibrium curves illustrated in Fig. 2.

Figure 3 shows how the intensity of the circulation modifies the vertical distributions of convective, radiative, and advective heating rates in the downdraught column. Figure 3(a) illustrates a moderate circulation intensity ($\Gamma = 4$), while Figs. 3(b) and (c) illustrate the two steady states, with and without deep convection, at $\Gamma = 360$. At $\Gamma = 4$, the radiative heating rate is nearly the same as in the local radiative–convective equilibrium; and the warming by subsidence is compensated by reduced convective heating. The heating rates shown in Fig. 3(b) are, qualitatively, representative for all equilibria beyond $\Gamma = 50$ that have deep convection in the downdraught column. Due to evaporation of rain in the mid-troposphere, the integrated convective heating is basically zero, and virtually no precipitation reaches the ground.

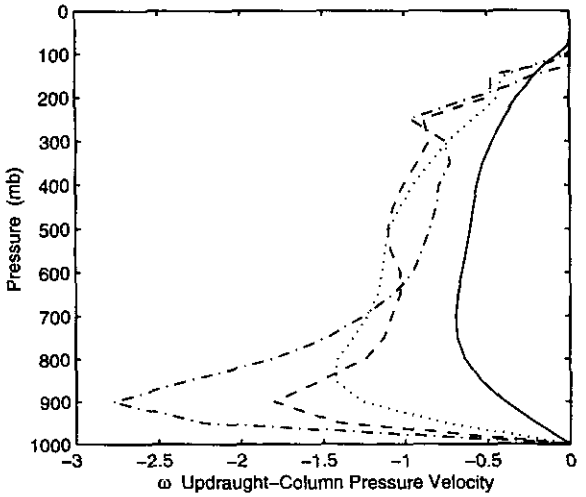

Figure 4. The updraught-column pressure velocity, ω, for equilibrium states with increasing flow intensity: flow parameter $\Gamma = 4$ (solid), $\Gamma = 50$ (dotted), $\Gamma = 360$ with deep convection (dashed), $\Gamma = 360$ without convection (dash-dotted). Here, ω is put in non-dimensional form using the scale ω_{rad} (see Eq. (25)), implying that unity approximates the rate of clear-sky subsidence in radiative–convective equilibrium. In the downdraught column, the pressure velocity is of equal magnitude but of the opposite sign. Note that ω is proportional to the stream function (see Eq. (9)).

(*b*) *The approach towards an inviscid atmosphere*

At a fixed column length, the flow parameter is essentially an inverse measure of the mechanical damping in the system. As the flow parameter increases, the interior atmosphere approaches an inviscid state, with nearly vanishing horizontal contrasts of virtual temperature (e.g. density). Viscous effects are, however, still of importance in a surface boundary layer. The formation of a viscous boundary layer is revealed clearly by the intensification of near-surface vertical velocity (see Fig. 4), which implies intense horizontal winds. In a horizontally resolved two-dimensional radiative–convective model, Held *et al.* (1993) obtain vertical distributions of velocity that are similar to the ones we obtain at large values of Γ. Their model also yields a strong near-surface maximum in the vertical velocity. The dissipation of kinetic energy per unit area, which is portrayed in Fig. 5, provides a different view of the formation of the viscous boundary layer. Along the branch with deep convection in both columns, the dissipation increases initially with Γ. Here, the intensity of the flow is limited partly by viscous effects. The enhanced dissipation that follows reduced mechanical damping reflects a general intensification of the atmospheric flow.

The general amplification of the circulation is halted when the vertical velocity in the mid-troposphere reaches the limit imposed by the radiative cooling in clear skies. In the interior atmosphere, the flow strength is now limited by thermal rather than viscous processes. Further reduction of the viscosity yields a rate of dissipation that, after an initial decline, becomes constant and independent of the damping. The height and velocity of the boundary layer adjust, for altered viscosity, in a way that keeps the dissipation of kinetic energy nearly invariant. Essentially, the same applies for the equilibrium states without convection in the downdraught column. Also, along that branch of steady states, the dissipation of kinetic energy is nearly independent of the viscosity. And the higher rates of dissipation simply reflect larger velocities.

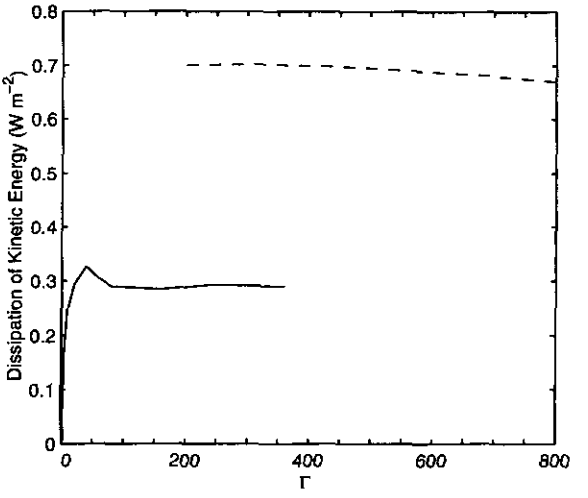

Figure 5. Dissipation of kinetic energy per unit area as a function of the flow parameter Γ for the equilibria with (solid line) and without convection (dashed line) in the downdraught column. If the column length is fixed, Γ is inversely proportional to the viscosity, which shows that the dissipation increases with decreasing viscosity, initially.

(*c*) *The horizontal redistribution of moist static energy and the radiator fin*

We now focus on why the large-scale circulation produces a colder equilibrium climate in the two-column model. As emphasised by Pierrehumbert (1995), this question is tied closely to the ability of the atmospheric circulation to create dry pools of air in regions of large-scale descent. From the dry regions, the infrared radiation can be exported to space more efficiently. It is not obvious, however, that the overturning circulation, which dries the downdraught column but moistens the updraught column, always should cool the climate of our model. One can speculate on different climate regimes with very dry atmospheres in which the advective moistening of the updraught column will dominate the change in atmospheric emissivity. We have conducted some simulations where the precipitation efficiency of our convection scheme has been increased, as well as simulations with a relatively low SST (10 °C). In these cases, the model produces dry atmospheres but the overturning circulation still cools the climate. Thus, it seems that rather drastic changes in the micro-physical features of cumulus convection are required before the large-scale circulation would warm the climate, at least in the present model.

To begin with, it is instructive to consider how the large-scale circulation affects the distributions of moisture and radiative heating in our model. Figures 6 and 7 illustrate the vertical distributions of relative humidity and radiative heating rates for varying intensity of the circulation. In the downdraught column, where the intensity of the convection decreases with the circulation, the advective drying is pronounced and affects the whole troposphere. The situation is quite different in the updraught column, where the flow acts essentially to moisten the atmosphere, and the intensity of the convection increases with the circulation. Here, the flow hardly affects the relative humidity of the lower troposphere. Note that intense flow actually dries the mid-troposphere.

The radiative heating rates are influenced by the flow chiefly via the changes in the vertical distributions of water vapour, which is the major infrared absorber in our clear-sky radiation calculation. As the downdraught column gets drier, the opacity of

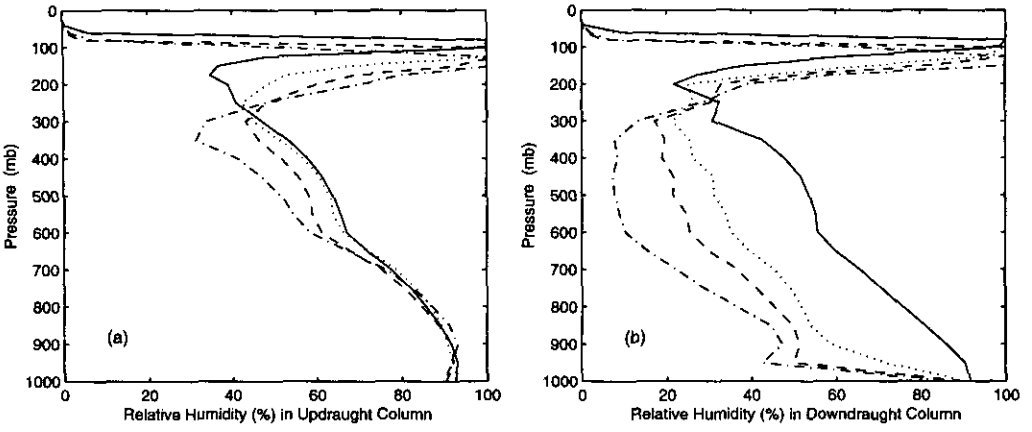

Figure 6. Profiles of relative humidity in (a) the updraught column and (b) the downdraught column. The family of profiles delineates the effect of increasing flow on the distribution of moisture. Here, the equilibrium profiles for flow parameter $\Gamma = 4$ (solid), $\Gamma = 50$ (dotted), $\Gamma = 360$ with deep convection (dashed), and $\Gamma = 360$ without convection (dash-dotted) are illustrated. Initially, the specific humidity in the stratosphere and upper troposphere is set to 0.002 g kg^{-1}. Transient bursts of convection can moisten the lower stratosphere, which then remains moist as our model essentially keeps the humidity constant above the convective layer. This causes the irregularities of the humidity profiles near the top of the convecting layer.

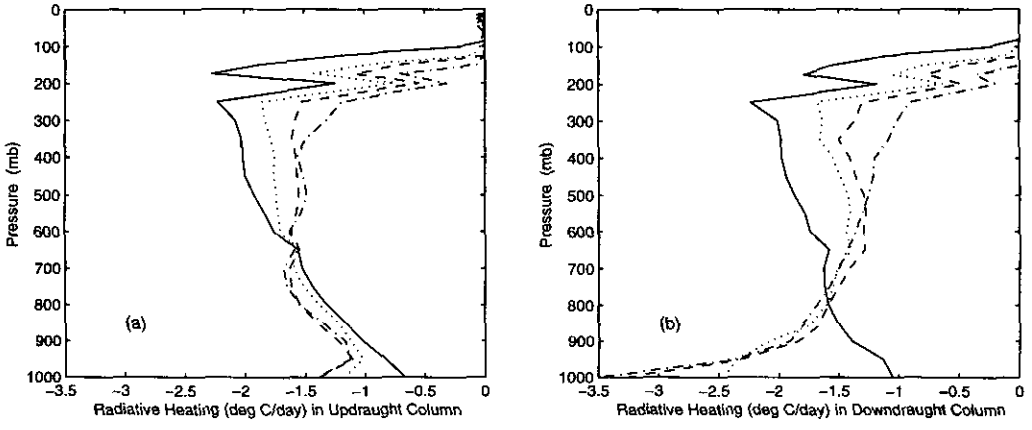

Figure 7. As in Fig. 6 but for profiles of radiative heating. Note that impact of flow on the radiative heating is less pronounced in the updraught column (a) than in the downdraught column (b). As clear-sky conditions are used in the radiation calculation (and the distributions of CO_2, ozone and other absorbers are fixed), the changes in the radiative heating rate are attributed chiefly to flow-induced changes in the distribution of water vapour. Qualitatively, the radiative-heating profiles of the circulating equilibrium at flow parameter $\Gamma = 4$ (solid line) and the local radiative–convective equilibrium are similar.

the atmosphere to infrared radiation is reduced. The bulk of the emission of radiation to space originates deeper down in the troposphere. As a consequence, the radiative cooling rate is enhanced in the lower troposphere while it is reduced in the upper troposphere (see Fig. 7(b)). In the updraught column, the response of the radiative heating rate to the flow exhibits a similar pattern, however, much less pronounced. Also, here the near-surface radiative cooling rate tends to increase with the flow. Still, even for intense flows, the profile of radiative cooling (which increases upward in the troposphere) is characteristic of an optically thick atmosphere.

Let us consider physically how the flow, via changes in the distribution of moisture, affects the equilibrium temperature. To bring out the essential physics, it is illuminating to introduce two conceptual simplifications. First, we neglect the very small horizontal temperature contrast in the interior troposphere (which here is always much smaller than the SST contrast). Fundamentally, this is an approximation of dynamical origin that is used frequently in treatments of the tropical circulation (see e.g. Pierrehumbert (1995) and Emanuel (1995)). Consequently, differences in infrared radiation between the columns are attributable almost solely to differences in the distributions of moisture. Second, as a leading order description, we assume that the flow-induced changes in the moisture distributions affect only the emission of infrared radiation from the downdraught column; this is supported by Fig. 7. (Strictly speaking, the emissivity of an atmosphere with a fixed profile of relative humidity changes with temperature as the specific humidity changes. In our model, however, the changes in emissivity of the downdraught column dominates. Here, the outgoing long-wave radiation increases with circulation despite the fact that the temperature declines.) We emphasise also that in our model, the net fluxes of solar radiation at the top of the two columns are virtually identical, and that these fluxes are essentially independent of the circulation.

The circulation-induced cooling of the equilibrium climate is elucidated by thinking of a time-dependent scenario. Suppose that we introduce a large-scale flow in a model atmosphere that is in radiative–convective equilibrium. To begin with, the flow dries the downdraught column, which increases its emission of infrared radiation. As a result, the downdraught column cools. In the updraught column, on the other hand, the net emission of infrared radiation is not affected directly by the flow. However, since the horizontal heat exchange is effective enough to wipe out any lateral temperature contrast, the updraught column is forced to trace the temperature decline of the downdraught column. As the system gets colder, the net emission of infrared radiation to space decreases gradually. Finally, a new equilibrium with large-scale circulation is attained, in which essentially the same amount of absorbed solar radiation is radiated to space by a colder but effectively more emissive atmosphere.

As the circulation hardly affects the emissivity of the updraught column, the lower temperature of the circulating equilibrium has now reduced the outgoing long-wave radiation there. Still, the updraught column absorbs essentially the same amount of solar radiation as in the local equilibrium. The excess of absorbed radiation is exported by the large-scale circulation from the updraught column to the dry, downdraught column, where it is radiated to space. In the words of Pierrehumbert (1995), the downdraught column acts as a radiator fin. Figure 8 illustrates how the column exchange of moist static energy depends on the parameter Γ. The circulation is thermally direct as it transports moist static energy out of the warm updraught column. Essentially, the maximum exchange of moist static energy is controlled by how large a column contrast in water vapour the model can produce, as this determines the column difference in upwelling infrared radiation.

(*d*) *Decoupling of the subcloud layer in the downdraught column*

The statistical equilibrium paradigm of convection, as advocated by Emanuel *et al.* (1994), presents a useful way to think about the interaction between convection and large-scale flows. A central argument of Emanuel *et al.* is that the convective processes are rapid enough to force the atmosphere to a state that is essentially neutral to convection. The observational study of Xu and Emanuel (1989) shows that the convectively neutral state can be approximated as an atmosphere with a moist adiabatic temperature

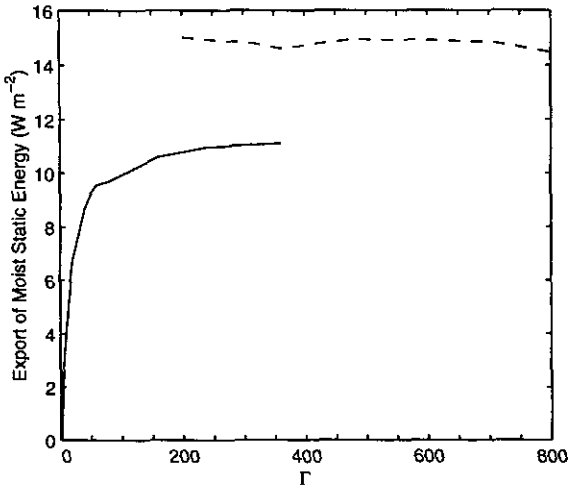

Figure 8. The export of moist, static energy from the updraught to the downdraught column, as a function of the parameter Γ. The solid line represents the equilibria with deep convection in both columns, and the dashed line represents the equilibria without deep convection in the downdraught column. As the system is in steady state, implying zero net heat flux across the sea surface, the export of moist static energy equals the net downward/upward radiative flux at the top of the updraught/downdraught column.

lapse rate—that is, the saturated entropy is constant with height above the cloud base and its value is determined by the entropy of the subcloud layer.

Provided that the subsidence of the large-scale flow is weak compared to the radiatively forced subsidence between clouds, the entropy of the subcloud layer essentially controls the temperature of the atmosphere aloft. In regions of strong subsidence, however, a trade inversion may form, which disconnects the boundary layer from the interior atmosphere. Above the trade inversion, the temperature lapse rate is still expected to be nearly moist adiabatic; however, the temperature is now controlled, via dynamical processes, by the subcloud entropy in the ascending branch of the circulation.

In our model, the surface boundary layer disconnects from the free atmosphere when the convection ceases in the downdraught column. The decoupling is revealed by an increase in the column difference in enthalpy (which is roughly proportional to the difference in entropy) of near-surface air (see Fig. 9). For the steady states with deep convection in the downdraught column, the boundary layer is never strictly disconnected from the free atmosphere. However, the causality of the interaction between the subcloud layer and the troposphere is, in essence, reversed as the system approaches the inviscid limit. Initially, when the circulation is weak and the convection nearly balances the radiative cooling, it is relevant to think that the subcloud enthalpy controls the stratification aloft. For stronger circulation, the heat budget of the downdraught column is shifted towards a balance between warming by subsidence and radiative cooling. Through dynamical processes, the stratification in the downdraught column becomes, to an increasing extent, controlled by the stratification in the updraught column, which is still forced to be nearly neutral to moist convection. In the inviscid limit, the stratification in the downdraught column is determined by the dynamical constraint that the horizontal difference in virtual temperature vanishes in the interior atmosphere. A manifestation of the dynamical constraint on the downdraught-column stratification is perhaps the decrease in the surface enthalpy difference with Γ as it exceeds 50 (see Fig. 9). Now increasing the flow parameter, which makes the system less viscid, reduces

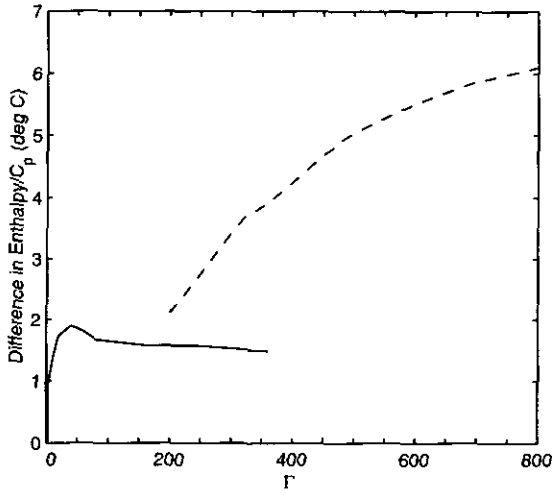

Figure 9. The near-surface, difference in moist enthalpy (i.e. $c_p T + L_v q$) between the two columns as a function of the parameter Γ (see text for definition of symbols). Along the branch representing equilibria with deep convection in the downdraught column (solid line), the near-surface, enthalpy difference reflects essentially the horizontal virtual-temperature contrasts of the free atmosphere.

the virtual-temperature difference in the free atmosphere. As some convection occurs in both columns, the difference in near-surface enthalpy has to decline with the interior contrasts in virtual temperature.

5. Discussion

(*a*) *Interaction between overturning circulations and infrared radiation in horizontally continuous models*

In our idealized model, the feedback between large-scale circulation, clear-sky water vapour, and radiation has the potential to destabilize the radiative–convective equilibrium. As this occurs, the model attains a new equilibrium with a thermally direct circulation that transports heat from the moist updraught column to the dry downdraught column. An obvious limitation of a two-column model is that the horizontal scale has to be specified. Also, we dictate that the ascending and descending columns have equal areas. For a fixed mechanical damping, the horizontal scale determines (via the parameter Γ) the strength of the circulation–radiation feedback and, therefore, the character of the equilibrium atmosphere. Thus, an important question that our study has left open is which scale the feedback between large-scale circulation and radiation selects in a model with a large number of side-by-side columns (or horizontal grid points). A related question is the determination of the relative area of subsiding and convecting regions in such a model.

To discuss these questions, it is instructive to translate the results of the linear stability discussion in section 3(d) to growth rates of horizontal wave-like disturbances in a continuous model. In this framework, Γ (which scales as $\mathcal{L}^{-2}$) is proportional to the square of the wave number, and the growth rate of perturbations is proportional to $\Gamma - 1$ (see Eq. (21)). Thus, the physical processes we have included in the conceptual model stabilize the largest scale, but give growth rates which, without limit, increase with the wave number. The low-wave-number cut-off of the instability occurs at the scale where the positive feedback between circulation, water vapour, and radiation

(which increases with wave number in our parametrization) is equal to the (scale-independent) negative feedbacks that act to restore the radiative–convective equilibrium. These negative feedbacks are tied to the temperature dependence of the outgoing long-wave radiation (OLR) and the surface heat exchange (in a model with fixed SST).

In reality, many processes can be conceived that curtail the circulation–radiation feedback at small scales. An important and perhaps dominating process is horizontal mixing of water vapour and hydrometeors. At sufficiently small scales, horizontal mixing prevents the subsiding regions from getting dry and, thereby, stabilizes the atmosphere. It is worth emphasizing that horizontal mixing is represented neither in our numerical model nor in our conceptual model. When horizontal mixing is taken into account, we expect that the circulation–radiation feedback tends to favour the emergence of large-scale circulation patterns that correspond, approximately, to the fastest growing perturbation. Here, the most unstable perturbation is associated with the scale that minimizes the negative feedbacks related to the temperature dependence of the OLR (damping the large scale) and the horizontal mixing of water vapour (damping the small scale). Clearly, strong negative feedbacks may make the circulation–radiation feedback insignificant regardless of the spatial scale.

An interesting study by Held *et al.* (1993) throws some light on the issues disussed above. They study radiative–convective equilibria in a periodic two-dimensional domain with moist convection explicitly calculated by a cloud model. In their model, the interaction between clouds and radiation is incorporated, and the dynamics is non-rotating and non-hydrostatic. A fixed SST provides the thermodynamic boundary condition at the bottom of the atmosphere. Depending on the treatment of the horizontal velocity, Held *et al.* (1993) obtain radically different patterns of convection. For cyclic boundary conditions, the model produces strong horizontal winds with significant shear and the convection is intermittent in space and time. On average, however, the convection occurs homogeneously in the domain. When the mean horizontal wind is forced to vanish, the convection collapses, finally, to a single location. In this case, the equilibrium is essentially time independent and is associated with a circulation that descends in the bulk of the model domain. For this equilibrium of Held *et al.* (1993), the thermally direct circulation presumably compensates for an imbalance in the top-of-the-atmosphere radiative flux, which is related to the difference in opacity to radiation between the convecting and the subsiding regions (Held, personal communication).

To some extent, we believe that the model behaviour reported by Held *et al.* (1993) can be interpreted in terms of different intensities of horizontal mixing of water vapour. For cyclic boundary conditions, the strong horizontal wind and the travelling convective activity result in an efficient mixing of water vapour. This prevents the development of an appreciable contrast in radiative characteristics (humidity and cloudiness) between convecting and subsiding regions. We speculate that a large-scale circulation pattern may be established also in this case, if the model domain is increased. Obviously, this requires that the circulation–radiation feedback does not reach its low-wave-number cut-off before the horizontal mixing of water vapour becomes negligible. If an equilibrium with a large-scale circulation is attained, however, we expect broader regions of mean ascent that contain several convective updraughts, but the descending regions would presumably still fill the bulk of the domain. The simulation of Held *et al.* (1993) without horizontal mean winds, where the convection is localized to a single spot, may serve to illustrate the limit of weak water-vapour mixing. In this limit, the localization of convection to the smallest resolved scale should be a general feature.

In any event, the study of Held *et al.* (1993) illustrates that the establishment of a steady large-scale circulation in a uniformly forced radiative–convective environment

is a delicate matter, even in a rather idealized model configuration. In nature and in complex models, a myriad of processes may reduce or obscure the feedback between circulation, water vapour, and infrared radiation that our simple model emphasizes. Aqua planet models, for example, generally produce strong variability in the form of propagating convective disturbances (e.g. Numaguti and Hayashi 1991a,b; Raymond and Torres 1998). These convection patterns act as travelling sources of moisture and should impede the establishment of large-scale dry regions. Also, the circulation–radiation feedback should be weak compared to the ocean–atmosphere feedbacks that are at the heart of the long-term variability and the climatology of the maritime Tropics (e.g. Philander 1990; Dijkstra and Neelin 1995; Neelin *et al.* 1998).

(*b*) *Climate sensitivity of the two-column model*

We conclude with a brief discussion of the climate sensitivity of the two-column model to changes in solar forcing. Here, the main purpose is to illustrate how the feedback between large-scale circulation, clear-sky water vapour, and infrared radiation affects the sensitivity in the minimal framework of a two-column model. Figures 10(a) and (*b*) portray the changes in SST and column exchange of moist static energy, respectively, caused by a change in solar radiation of 5 W m^{-2} as a function of Γ. To begin with, consider the model atmospheres with a vanishingly weak circulation (Γ of the order of unity), which respond to climate forcing approximately as a single-column model of radiative–convective equilibrium. As this model ignores cloud–radiative feedbacks, the sensitivity is essentially determined by the rate at which the clear-sky OLR increases with temperature. Rennó *et al.* (1994b) discuss in detail the physical processes that determine the sensitivity of the radiative–convective equilibrium with reference to the present radiative–convective code.

When the overturning circulation can no longer be ignored in the heat balance, the feedback between circulation, water vapour, and infrared radiation reduces the model sensitivity. In essence, the sensitivity of the equilibria with a large-scale circulation is diminished by two effects. First of all, the overturning circulation dries the atmosphere, which results in a sharper increase in clear-sky OLR with temperature. Second, an increase in solar forcing tends to enhance the positive feedback between circulation

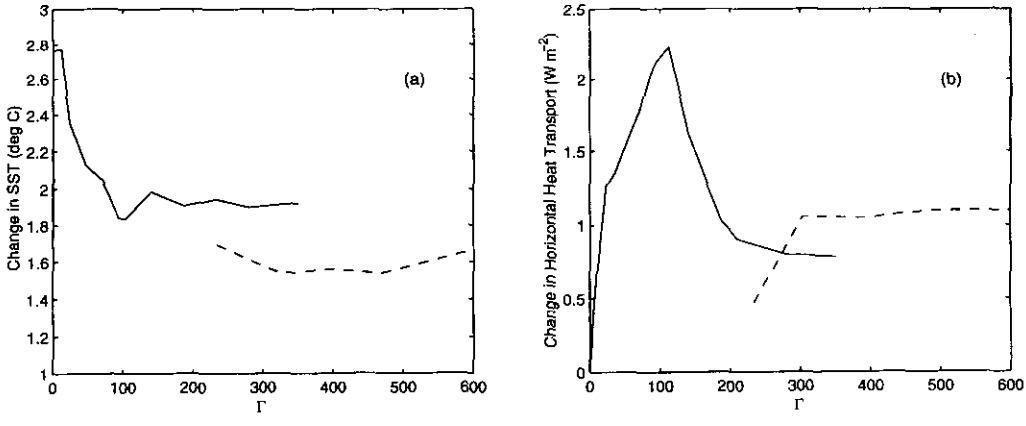

Figure 10. Changes in (a) mean SST and (b) horizontal transport of moist static energy, as functions of the flow parameter Γ caused by a change in insolation of 5 W m^{-2}. The solid and dashed lines represent equilibria with and without deep convection in the downdraught column, respectively.

and radiation, which intensifies the circulation and further reduces the relative humidity. If the columns were thermally disconnected, the moist updraught column would have to warm more than the dry downdraught column to emit the surplus solar radiation. As the thermal communication between the columns is efficient, the tendency to separate the temperature of the columns forces a stronger circulation, which essentially keeps the temperature horizontally uniform above the boundary layer. This feedback is most pronounced for some intermediate values of Γ (see Fig. 10(b)). Here, the equilibria with a weaker insolation have a circulation which has not quite reached the limit imposed by the radiatively forced subsidence in clear skies. The increase in solar forcing allows the vertical velocity in the mid-troposphere to approach its full strength.

As the strength of the circulation in the mid-troposphere becomes comparable to the clear-sky radiatively forced subsidence, the relative-humidity distribution of the model approaches an asymptotic form (see Fig. 6). When this occurs (near $\Gamma = 100$), the influence of Γ on the equilibrium atmospheres becomes weak. Here, the model can be conceptualized as two columns of equal temperature (above the boundary layer) with fixed but different profiles of relative humidity. The intensification of moist static energy transport with solar forcing is essentially dictated by the difference in infrared emissivity between the columns, which in turn is determined by the column contrast in humidity. As expected, the very dry equilibrium atmospheres without convection in the downdraught column have the weakest sensitivity.

Despite its obvious limitations, we believe that our study is instructive in isolating how the feedback between large-scale circulation and clear-sky water vapour affects the climate sensitivity when the horizontal homogeneity of radiative–convective equilibrium is relaxed. Admittedly, a vast number of processes of importance to the sensitivity of the real climate are missing in our model. Here, we point at three fundamental processes that can be included, and perhaps illuminated, in a slightly modified version of the present model. First, as emphasised by Pierrehumbert (1995), changes in climate forcing may result in an alteration of the relative area of convecting and subsiding regions. A radiative–convective model with a couple of side-by-side columns may serve as a starting point to study this potentially important mechanism of climate regulation. Second, cloud–radiative feedbacks may strongly modify the sensitivities produced by our clear-sky model. Miller (1997), for example, studies the ability of low stratus clouds to moderate the tropical climate (using a three-column model with implicit dynamics and convection). When the low cloud cover in his model is allowed to respond to a doubling of CO_2, the increase in SST is curtailed by up to 50% relative to simulations with a fixed cloud cover. Cloud–radiative feedbacks, however, appear to be a delicate issue. In some model studies, the interaction between clouds and radiation tends to amplify the climate forcing (e.g Meehl and Washington 1996). In any event, it would be interesting to include cloud–radiative feedbacks in the present model using, for example, the cloud parametrization of Miller (1997). Finally, feedbacks between winds and oceanic heat transport appear to be important for the sensitivity of the tropical climate (e.g. Clement *et al.* 1996; Sun and Liu 1996; Seager and Murtugudde 1997; Liu and Huang 1997). In an ongoing work, we plan to study ocean–atmosphere feedbacks that pertain to the climatology and sensitivity of the Tropics with the present two-column model coupled to a dynamically active two-box ocean model.

ACKNOWLEDGEMENTS

This research is supported by the Swedish Natural Science Research Council and the National Ocean Atmosphere Administration.

REFERENCES

Asselin, R. 1972 Frequency filter for time integrations. *Mon. Weather Rev.*, **100,** 437–490

Chou, M.-D 1992 A solar radiation model for use in climate studies. *J. Atmos. Sci.*, **49,** 762–772

Chou, M.-D., Krats, D. P. and Ridgway, W. 1991 Infrared radiation parameterization in numerical climate models. *J. Climate*, **4,** 424–437

Clement, A. C., Seager, R., Cane, M. A. and Zebiak, S. E. 1996 An ocean dynamical thermostat. *J. Climate*, **9,** 2190–2196

Dijkstra, H. A. and Neelin, J. D. 1995 Ocean–atmosphere interaction and the tropical climatology. Part II: Why the Pacific cold tongue is in the east. *J. Climate*, **8,** 1343–1359

Emanuel, K. A. 1987 An air–sea interaction model of intraseasonal oscillations in the tropics. *J. Atmos. Sci.*, **42,** 2324–2340

1991 A scheme for representing cumulus convection in large-scale models. *J. Atmos. Sci.*, **48,** 2313–2335

1994 *Atmospheric convection.* Oxford University Press

1995 On thermally direct circulations in moist atmospheres. *J. Atmos. Sci.*, **52,** 1530–1534

Emanuel, K. A., Neelin, J. D. and Bretherton, C. S. 1994 On large-scale circulations in convecting atmospheres. *Q. J. R. Meteorol. Soc.*, **120,** 1111–1143

Gill, A. E. 1982 *Atmosphere–ocean dynamics.* Academic Press, New York

Held, I. M., Helmer, R. S. and Ramaswamy, V. 1993 Radiative–convective equilibrium with explicit two-dimensional moist convection. *J. Atmos. Sci.*, **50,** 3909–3927

Lindzen, R. S. and Nigam, S. 1987 On the role of sea surface temperature gradients in forcing low-level wind and convergence in the tropics. *J. Atmos. Sci.*, **44,** 2418–2436

Liu, Z. and Huang, B. 1997 A coupled theory of tropical climatology: Warm pool, cold tongue, and Walker circulation. *J. Climate*, **10,** 1662–1679

Marotzke, J. and Pierce, W. P. 1997 On spatial-scales and lifetimes of SST anomalies beneath a diffusive atmosphere. *J. Phys. Oceanogr.*, **27,** 133–139

Meehl, G. A. and Washington, W. M. 1996 El Niño-like climate change in a model with increased atmospheric CO_2 concentrations. *Nature*, **382,** 56–60

Miller, R. L. 1997 Tropical thermostats and low cloud cover. *J. Climate*, **10,** 409–440

Neelin, J. D. 1989 On the interpretation of the Gill model. *J. Atmos. Sci.*, **46,** 2466–2468

Neelin, J. D. and Held, I. M. 1987 Modelling tropical convergence based on moist static energy budgets. *Mon. Weather Rev.*, **115,** 3–12

Neelin, J. D. and Yu, J.-Y. 1994 Modes of tropical variability under convective adjustment and the Madden–Julian oscillation. Part I: Analytical theory. *J. Atmos. Sci.*, **51,** 1876–1894

Neelin, J. D., Held, I. M. and Cook, K. H. 1987 Evaporation–wind feedback and low-frequency variability in the tropical atmosphere. *J. Atmos. Sci.*, **44,** 2341–2348

Neelin, J. D., Battisti, D. S., Hirst, A. C., Jin, F.-F., Wakata Y., Yamagata T. and Zebiak, S. E. 1998 ENSO theory. *J. Geophys. Res.*, **103 (C7),** 14261–14290

Numaguti, A. and Hayashi, Y.-Y. 1991a Behavior of cumulus activity and the structures of circulation in an 'aqua planet' model. Part I: The structure of the super clusters. *J. Meteorol. Soc. Jpn.*, **69,** 541–561

1991b Behavior of cumulus activity and the structures of circulation in an 'aqua planet' model. Part II: Eastward moving planetary scale structure. *J. Meteorol. Soc. Jpn.*, **69,** 563–579

Philander, S. G. H. 1990 *El Niño, La Niña, and the southern oscillation.* Academic Press, New York

Pierrehumbert, R. T. 1995 Thermostats, radiator fins, and the local runaway greenhouse. *J. Atmos. Sci.*, **52,** 1784–1806

Ramanathan, V., Cess, R. D., Harrison, E. F., Minnis, P., Barkstrom, B. R., Ahmad, E. and Hartman, D. 1989 Cloud–radiative forcing and climate: Results from the earth radiation budget experiment. *Science*, **243,** 57–63

Raymond, J. R. and Torres, D. J. 1998 Fundamental moist modes of the equatorial troposphere. *J. Atmos. Sci.*, **55,** 1771–1790

Rennó, N. O. 1997 Multiple equilibria in radiative–convective atmospheres. *Tellus*, **97A,** 423–438

Rennó, N. O., Emanuel, K. A. and Stone P. H.	1994a	Radiative–convective model with an explicit hydrological cycle. Part I: Formulation and sensitivity to model parameters. *J. Geophys. Res.*, **99 (D7),** 14429–14441
Rennó, N. O., Stone P. H. and Emanuel, K. A.	1994b	Radiative–convective model with an explicit hydrological cycle. Part II: Sensitivity to large changes in the solar forcing. *J. Geophys. Res.*, **99 (D8),** 17001–17020
Seager, R. and Murtugudde, R.	1997	Ocean dynamics, thermocline adjustment, and regulation of tropical SST. *J. Climate*, **10,** 521–534
Seager, R., Kushnir, Y. and Cane, M. A.	1995	On heat flux boundary conditions for ocean models. *J. Phys. Oceanogr.*, **25,** 3219–3230
Sherwood, S. C.	1996	Maintenance of the free-tropospheric tropical water vapor distribution. Part II: Simulation by large-scale advection. *J. Climate*, **9,** 2919–2934
Sun, D. and Liu, Z.	1996	Dynamic ocean–atmosphere coupling: A thermostat for the Tropics. *Science*, **272,** 1148–1150
Xu, K. and Emanuel, K. A.	1989	Is the tropical atmosphere conditionally unstable? *Mon. Weather Rev.*, **121,** 21–36
Yu, J.-Y. and Neelin, J. D.	1997	Analytic approximations for moist convectively adjusted regions. *J. Atmos. Sci.*, **54,** 1054–1063
Yu, J.-Y., Chou, C. and Neelin, J. D.	1998	Estimating the gross moist stability of the tropical atmosphere. *J. Atmos. Sci.*, **55,** 1354–1372